ISSN 1674-1056
http://cpb.iphy.ac.cn
http://iopscience.iop.org/cpb
中国物理 B
Chinese Physics
中国物理
Chinese Physics B

Stochastic resonance and synchronization behaviors of excitatory-inhibitory small-world network subjected to electromagnetic induction

Xiao-Han Zhang(张晓函), Shen-Quan Liu(刘深泉)
Citation: Chin. Phys. B . 2018, 27(4): 040501. **doi:** 10.1088/1674-1056/27/4/040501

Journal homepage: http://cpb.iphy.ac.cn; http://iopscience.iop.org/cpb

What follows is a list of articles you may be interested in

A new four-dimensional chaotic system with first Lyapunov exponent ≈ 22, hyperbolic curve and circular paraboloid types of equilibria and its switching synchronization by an adaptive global integral sliding mode control

Jay Prakash Singh, Binoy Krishna Roy, Zhouchao Wei(魏周超)
Chin. Phys. B . 2018, 27(4): 040503. **doi:** 10.1088/1674-1056/27/4/040503

Stochastic resonance and synchronization behaviors of excitatory-inhibitory small-world network subjected to electromagnetic induction

Xiao-Han Zhang(张晓函), Shen-Quan Liu(刘深泉)
Chin. Phys. B . 2018, 27(4): 040501. **doi:** 10.1088/1674-1056/27/4/040501

Linear synchronization and circuit implementation of chaotic system with complete amplitude control

Chun-Biao Li(李春彪), Wesley Joo-Chen Thio, Julien Clinton Sprott, Ruo-Xun Zhang(张若洵), Tian-Ai Lu(陆天爱)
Chin. Phys. B . 2017, 26(12): 120501. **doi:** 10.1088/1674-1056/26/12/120501

Free-matrix-based time-dependent discontinuous Lyapunov functional for synchronization of delayed neural networks with sampled-data control

Wei Wang(王炜), Hong-Bing Zeng(曾红兵), Kok-Lay Teo
Chin. Phys. B . 2017, 26(11): 110503. **doi:** 10.1088/1674-1056/26/11/110503

Generalized analytical solutions for certain coupled simple chaotic systems

G Sivaganesh, A Arulgnanam
Chin. Phys. B . 2017, 26(5): 050502. **doi:** 10.1088/1674-1056/26/5/050502

Stochastic resonance and synchronization behaviors of excitatory-inhibitory small-world network subjected to electromagnetic induction*

Xiao-Han Zhang(张晓函) and Shen-Quan Liu(刘深泉)†

School of Mathematics, South China University of Technology, Guangzhou 510640, *China*

(Received 23 October 2017; revised manuscript received 9 January 2018; published online 10 March 2018)

The phenomenon of stochastic resonance and synchronization on some complex neuronal networks have been investigated extensively. These studies are of great significance for us to understand the weak signal detection and information transmission in neural systems. Moreover, the complex electrical activities of a cell can induce time-varying electromagnetic fields, of which the internal fluctuation can change collective electrical activities of neuronal networks. However, in the past there have been a few corresponding research papers on the influence of the electromagnetic induction among neurons on the collective dynamics of the complex system. Therefore, modeling each node by imposing electromagnetic radiation on the networks and investigating stochastic resonance in a hybrid network can extend the interest of the work to the understanding of these network dynamics. In this paper, we construct a small-world network consisting of excitatory neurons and inhibitory neurons, in which the effect of electromagnetic induction that is considered by using magnetic flow and the modulation of magnetic flow on membrane potential is described by using memristor coupling. According to our proposed network model, we investigate the effect of induced electric field generated by magnetic stimulation on the transition of bursting phase synchronization of neuronal system under electromagnetic radiation. It is shown that the intensity and frequency of the electric field can induce the transition of the network bursting phase synchronization. Moreover, we also analyze the effect of magnetic flow on the detection of weak signals and stochastic resonance by introducing a subthreshold pacemaker into a single cell of the network and we find that there is an optimal electromagnetic radiation intensity, where the phenomenon of stochastic resonance occurs and the degree of response to the weak signal is maximized. Simulation results show that the extension of the subthreshold pacemaker in the network also depends greatly on coupling strength. The presented results may have important implications for the theoretical study of magnetic stimulation technology, thus promoting further development of transcranial magnetic stimulation (TMS) as an effective means of treating certain neurological diseases.

Keywords: electromagnetic induction, synchronization, stochastic resonance, small-world network

PACS: 05.40.–a, 05.45.–a, 87.85.Ng, 87.85.dq **DOI:** 10.1088/1674-1056/27/4/040501

1. Introduction

Biological nervous system comprises a large number of neurons, of which the neurodynamics has been extensively studied. Moreover, some biological neuron models have been established, which is helpful in understanding mode transition in electric activities. The Hodgkin–Huxley[1] and Morris–Lecar[2] neuron models can be used to describe the effect of ion channels, which are thought of as a reliable neuron model. A discrete map-type model was recently proposed by Rulkov,[3] which can produce the main properties of neuronal activities despite its low dimensionality and intrinsic simplicity.[4] The mathematical Hindmarsh–Rose neuron model, which is simplified by the original Hodgkin–Huxley neuron model, can reproduce the dynamical properties in neuronal activities and model the bifurcation behaviors of neurons.[3,4] A detailed description of other models can be found in Ref. [7] However, because neurodynamics in biological system are much too complex, many factors need considering in the neuronal model. According to the Faraday's electromagnetic induction law, the fluctuation over time in internal action potentials in neurons can produce a magnetic field, which changes the distribution of electromagnetic fields inside and outside the neuron. Therefore, the electromagnetic effect should be considered. Lv *et al.* suggested that the magnetic flux across the membrane can be used to describe the effect of electromagnetic induction.[8,9]

In the past few decades, many experimental and theoretical studies have focussed on synchronous oscillations in neural systems.[10] Gu *et al.* investigated the influences of bursting on the control parameter, initial value, and attraction domain on synchronization transition processes of coupled neurons.[11,12] A prevailing view is that some neurological diseases and numerous cognitive functions are related to neuronal oscillations. For example, some studies show that the cortical gamma rhythm is associated with memory[13] and movement.[14] Moreover, abnormal synchronous gamma oscillations occur in patients with Alzheimer's disease[15,16] and autism.[17] More recently, Wang and Zhang studied the effect of phase synchro-

*Project supported by the National Natural Science Foundation of China (Grant No. 11172103).

†Corresponding author. E-mail: mashqliu@scut.edu.cn

© 2018 Chinese Physical Society and IOP Publishing Ltd

nization in neural information transmission.[18] Jiao and Wang investigated the synchronous discharge patterns of neuronal population, which are composed of excitatory and inhibitory connections.[19]

Moreover, the phenomenon of stochastic resonance has also been extensively studied.[20–22] For instance, Gong *et al*. studied the spatial synchronization and the temporal coherence of the stochastic Hodgkin–Huxley model on complex networks which are subjected to channel noise, and found that the temporal coherence and synchronization can be enhanced by randomly adding shortcuts.[23] The research of Gao *et al*. showed that the stochastic resonance effect and synchronization depend greatly on the coupling strength and rewiring probability in a small-world neural network.[24] Studies of neural networks reported that the stochastic resonance is very important for our understanding of the weak signal detection and information transmission.[25] Moerover, adding noise into the neuron system can significantly enhance the ability of sensory neurons to respond to weak input signals.[26,27] However, in all these studies, the dynamics of neural networks is based on the loading of weak periodic stimuli on each constitutive unit. Perc *et al*. introduced a subthreshold periodic pacemaker into a single unit of the network, which imposes the operating rhythm on adjacent cells to guide the functioning of the whole network.[28] Furthermore, they also investigated the phenomenon of stochastic resonance on small-world networks with a pacemaker.[29] Moreover, Wang *et al*. studied the phenomenon of pacemaker-driven stochastic resonance on excitable modular neural networks, which are composed of several subnetworks and driven only by one neuron.[30]

Neurons in the nervous system undergo multiple physiological processes, such as the influences of electrical field and magnetic flux across the membrane. The influence of an induced electric field on the rhythmic activity of the nervous network has been investigated. For example, transcranial magnetic stimulation (TMS) generates a magnetic field in an area of interest in the brain, which can modulate the neuronal activity in a particular brain tissue.[31] Devos and Lefebvre found the abnormal patterns of cortical oscillatory activity.[32] Ma jun *et al*. studied the synchronization behaviors of coupled neurons under electromagnetic radiation and found that the neuronal synchronization degree depends on the intensity of electromagnetic radiation.[33]

However, to the best of our knowledge, in the past there has been no corresponding work on studying the influence of the electromagnetic induction among neurons on the collective dynamics of the complex system. Therefore, in this paper, in order to explore this, we study the phenomenon of neuron population synchronization and pacemaker-driven stochastic resonance in a small-world network consisting of excitatory neurons and inhibitory neurons (we call it the E-I small-world network). More precisely, we construct a small-world network proposed by Watts and Strogatz.[34] The excitatory neuron and inhibitory neurons are modeled by a simple two-dimensional model proposed recently by Izhikevich,[35] which is as biologically plausible as the Hodgkin–Huxley model, but in terms of computational efficiency, it is like the integrate-and-fire model, thus allowing detailed dynamic analysis for large-scale network simulations. In particular, the effects of electromagnetic induction among neurons and external induced electric field are imposed on the model. The synaptic currents in the model are the AMPA and the GABA currents elicited by excitatory neurons and the inhibitory neurons, respectively. Using this E-I small-world network, we systemically study the influences of electromagnetic induction among neurons on pacemaker-driven stochastic resonance and the detection of weak signals. Moreover, the effect of electrical field induced by the magnetic stimulus on neuron population synchronization is also investigated.

2. Materials and methods

In this section, we will introduce the topology structure of the considered network, mathematical description of neurons, and synaptic model used by neurons coupling. In addition, the measurement network synchronization index is also introduced.

First, according to Faradays' law, a time-varying electric field will be induced when a magnetic field, which changes with time, is applied to the brain. Therefore, this electric field can also be determined. Moreover, the influence of induced electric field on membrane depolarization can be considered. We know that the membrane potential V is due to the difference in ion concentration between inside and outside the cell membrane. The effect of induction electric field on cell membrane potential is shown to change the concentrations of ions inside and outside the cell membrane, thus causing the membrane potential to change, and thus further affecting the firing patterns of neurons. Under the effect of induced electric field, charges will accumulate in some parts of the membrane. As charge accumulation increases, the depolarization of the membrane will be greater. The relationship between the electric field E and the electric field-induced membrane depolarization ΔV will satisfy the following differential equation:

$$\frac{\Delta V}{\mathrm{d}t} + \frac{\Delta V}{\tau} = \frac{\lambda}{\tau} E, \tag{1}$$

where λ is the polarization length and τ is the Maxwell–Wagner time constant, which represents the 'speed' of charge accumulation.[36] According to formula (1), when the external electric field is a direct current (DC) electric field, the corresponding membrane depolarization ΔV is

$$\Delta V = \lambda E. \tag{2}$$

For alternating current (AC) electric field $E(t) = (A/\omega)\sin(\omega t)$, where A and ω represent the amplitude and angular frequency respectively, the corresponding membrane depolarization ΔV is

$$\frac{\Delta V}{\lambda} = \frac{AV}{\omega}\frac{\sin(\omega t) - 2\pi f\tau\cos(\omega t)}{1+(\omega t)^2}. \tag{3}$$

Because τ is very small and its magnitude is 10^{-10}, while the frequency f is in an extremely low frequency range, so $\omega\tau \ll 1$, formula (3) can be rewritten as

$$\Delta V(t) = \lambda\frac{A}{\omega}\sin(\omega t). \tag{4}$$

Here, the polarization length is $\lambda = 1$ mm.

The field-induced membrane depolarization ΔV can be seen as an additive perturbation to the membrane potential V.[37] The neuron models of DC and AC electric field can be obtained by substituting the formulas (2) and (4) into the membrane potential equation respectively. In this study, we use V_e to represent ΔV.

2.1. Neuron dynamics

We use the single two-dimensional (2D) neuron model proposed by Izhikevich[35] to simulate the dynamics of individual neurons in the network, which can be expressed as

$$\begin{aligned} v' &= 0.04v^2 + 5v + 140 - u + I, \\ u' &= a(bv - u), \end{aligned} \tag{5}$$

with resetting the auxiliary after-spike condition:

$$\text{if } v \geq 30\text{ mV}, \quad \text{then } \begin{cases} v \leftarrow c, \\ u \leftarrow u + d, \end{cases} \tag{6}$$

where v and u represent the transmembrane voltage of the neuron and membrane recovery variable, respectively. The variable I represents the synaptic current or injected dc-current: a, b, c, and d are the dimensionless parameters. Through various choices of these parameter values, the model can show discharge patterns of all known types of cortical neurons. In this paper, we choose a regular spiking model (RS) as excitatory neurons, which corresponds to $a = 0.02$, $b = 0.2$, $c = -65$, and $d = 8$, and we choose low-threshold spiking model (LTS) as inhibitory neurons, which corresponds to $a = 0.1$, $b = 0.25$, $c = -50$, and $d = 8$.

2.2. E-I small-world network

According to the random rewiring procedure proposed by Watts and Strogatz,[34] we use the following methods to build a small-world network: starting from a ring-like network with regular connectivity, where each node is connected to its $2m$ nearest neighbors, then we rewire each edge at random with probability p. Self-connected and duplicate edges are forbidden. By increasing probability p, the construction of the network can be tuned between regularity $(p = 0)$ and disorder $(p = 1)$. As shown in Fig. 1, small-world networks can be characterized by intermediate region $0 < p < 1$. Generally, the topology can be viewed as a random one when $p > 0.3$.

Our small-world network consists of $N = 200$ neurons, including $N_e = 160$ excitatory neurons (E-cells) and $N_i = 40$ inhibitory neurons (I-cells). The dynamics of the individual neuron in the network is represented by following the improved regular spiking model and improved low-threshold spiking model.

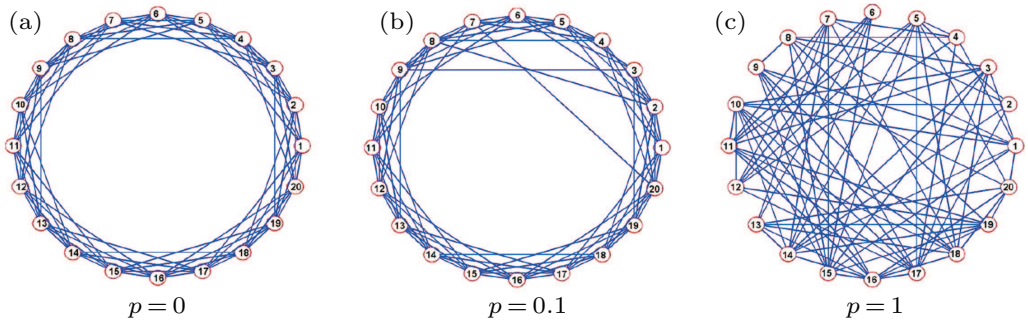


Fig. 1. (color online) Examples of considered small-world network topologies and only 20 isolated nodes are displayed in each panel, showing (a) regular ring-like network characterized by random rewiring probability $p = 0$, with each node being connected to its $m = 4$ nearest neighbors, (b) $p = 0.1$, and (c) $p = 1$.

2.3. Neuron model and synaptic model in network

Here, we consider a network with a small-world topology which is coupled by E-cells and I-cells. These excitatory neurons derive from the regular spiking model, and inhibitory neurons derive from the low-threshold spiking mentioned above. We use the improved regular spiking model as E-cells and the improved low-threshold spiking model as I-cells in the network, which contain the effects of electromagnetic induction among neurons and external electric field. Therefore, to describe the dynamical properties of neurons in the network, we only need to change Eq. (5) into the following form and the corresponding parameters a, b, c, d stay the same

$$\begin{cases} v' = 0.04(v+V_{\rm e})^2 + 5(v+V_{\rm e}) + 140 - u - k_1\rho(\varphi)(v+V_{\rm e}) \\ \quad -A_{\rm e} f\cos(ft) + I_{\rm syn} + I_{\rm b} + \xi(t), \\ u' = a(bv-u), \\ \varphi' = v - k_2\varphi, \\ \dfrac{{\rm d}q(\varphi)}{{\rm d}\varphi} = \rho(\varphi), \end{cases} \tag{7}$$

where $V_{\rm e} = A_{\rm e}\sin(ft)$ is an AC electric field, which can be seen as an additive perturbation to the membrane potential v, $A_{\rm e}$ is the amplitude of the electric field, and f is the frequency. This time, we change v into $v+V_{\rm e}$, and ${\rm d}V_{\rm e}/{\rm d}t = (A_{\rm e}\sin(ft))' = A_{\rm e} f\cos(ft)$. This is what the right side of Eq. (7) describes. The variable φ represents the magnetic flux across the membrane. The function $\rho(\varphi)$ is the memory conductance used to describe the relationship between magnetic field and membrane potential of the neuron, which develops from the magnetic flux-controlled memristor.[38] We often use $\rho(\varphi) = \alpha + 3\beta\varphi^2$ to describe the memory conductance of the memristor and the parameters α, β are fixed.[39] k_1 and k_2 are parameters that describe the interaction between the membrane potential and magnetic flux. The term $k_1\rho(\varphi)v$ represents the inhibitory regulation on the membrane potential. According to the definition of the memristor and Faraday law, we can think of the term $k_1\rho(\varphi)v$ as the induction current on the membrane, and the equation is as follows:

$$i' = \frac{{\rm d}q(\varphi)}{{\rm d}t} = \frac{{\rm d}q(\varphi)}{{\rm d}\varphi}\frac{{\rm d}\varphi}{{\rm d}t} = \rho(\varphi)V = k_1\rho(\varphi)v, \tag{8}$$

where $I_{\rm b}$ is the Brownian white noise term with mean $0.2uA$ and standard deviation $2uA$, which represents the nonspecific background current from other brain areas and $\xi(t)$ is the Gaussian white noise, which satisfies the following properties:

$$\langle\xi(t)\rangle = 0; \langle\xi(t)\xi(t')\rangle = 2D\delta(t-t'), \tag{9}$$

where $\delta(*)$ represents the Dirac-δ function, D is the noise intensity, $\langle*\rangle$ is the average of variable on time, and $I_{\rm syn}$ is the coupling term, the form of which depends on the small-world network topology.

The synaptic current elicited by E-cells is the AMPA and the synaptic current elicited by the I-cells is the GABA.[40] In E-cells model of the network, the form of $I_{\rm syn}$ is $I_{\rm AMPA}^{\rm E\to E} + I_{\rm GABA}^{\rm I\to E}$, and in I-cells, the form of $I_{\rm syn}$ is $I_{\rm AMPA}^{\rm E\to I} + I_{\rm GABA}^{\rm I\to I}$. For E-cells ($i \le N_{\rm e}$), the AMPA currents to both E-cells ($j \le N_{\rm e}$) and I-cells ($j > N_{\rm e}$) can be described by the following forms:

$$\begin{aligned} &I_{{\rm AMPA},j}^{\rm E\to E}(v, \{s_{\rm AMPA}\}) \\ &= g_{\rm AMPA}^{\rm E\to E}(v - V_{\rm Glu})\varepsilon_{\rm EE}\sum_{i=1}^{N_{\rm e}} M_{ij}s_{{\rm AMPA},i}, \end{aligned} \tag{10}$$

$$\begin{aligned} \frac{{\rm d}s_{{\rm AMPA},i}}{{\rm d}t} &= k_{\rm fp}T_{{\rm Glu},i}s_\infty(v_i)(1 - s_{{\rm AMPA},i}) \\ &\quad - s_{{\rm AMPA},i}/\tau_{\rm AMPA}, \end{aligned} \tag{11}$$

$$\frac{{\rm d}T_{{\rm Glu},i}}{{\rm d}t} = -k_t s_\infty(v_i)T_{{\rm Glu},i} + k_v(1 - T_{{\rm Glu},i}), \tag{12}$$

$$s_\infty(v_i) = (1 + \exp(-(v - (\theta_{\rm s})/\sigma_{\rm s}))), \tag{13}$$

$$\begin{aligned} &I_{{\rm AMPA},j}^{\rm E\to I}(v, \{s_{\rm AMPA}\}) \\ &= g_{\rm AMPA}^{\rm E\to I}(v - V_{\rm Glu})\varepsilon_{\rm EI}\sum_{i=1}^{N_{\rm e}} M_{ij}s_{{\rm AMPA},i}, \end{aligned} \tag{14}$$

where $\theta_{\rm s} = -20$ mV, $\sigma_{\rm s} = 2$ mV, $k_{\rm fp} = 1$ ms^{-1}, $k_t = 1$ ms^{-1}, $k_v = 0.0001$ ms^{-1}, $\tau_{\rm AMPA} = 5$ ms, $g_{\rm AMPA}^{\rm E\to E} = 0.08$ mS/cm^2, $g_{\rm AMPA}^{\rm E\to I} = 0.05$ mS/cm^2, and $V_{\rm Glu} = 0$ mV. The synaptic weight of E-cells-to-E-cells is $\varepsilon_{\rm EE} = 3$, and that of E-cells-to-I-cells is $\varepsilon_{\rm EI} = 1$.

For I-cells ($i > N_{\rm e}$) the GABA currents to both E-cells ($j \le N_{\rm e}$) and I-cells ($j > N_{\rm e}$) can be described as

$$\begin{aligned} &I_{{\rm GABA},j}(v, \{s_{\rm GABA}\}) \\ &= g_{\rm GABA}(v - V_{\rm GABA})\varepsilon\sum_{i=N_{\rm e}+1}^{N} M_{ij}s_{{\rm GABA},i}, \end{aligned} \tag{15}$$

$$\begin{aligned} &\frac{{\rm d}s_{{\rm GABA},i}}{{\rm d}t} \\ &= k_{\rm fa}s_\infty(v_i)(1 - s_{{\rm GABA},i}) - s_{{\rm GABA},i}/\tau_{\rm GABA}, \end{aligned} \tag{16}$$

where $k_{\rm fa} = 1$ ms^{-1}, $g_{\rm GABA} = 0.05$ mS/cm^2, $\tau_{\rm GABA} = 10$ ms, $V_{\rm GABA} = -70$ mV. ε is the synaptic weight, the weight of I-cells-to-E-cells is 3, and that of I-cells-to-I-cells is 1.

Here, M is the connectivity matrix: $M_{ij} = M_{ji} = 1$ if neuron i is connected to neuron j, $M_{ij} = M_{ji} = 0$ otherwise, and $M_{ii} = 0$. Obviously, the connectivity matrix M is asymmetric and sparse.

2.4. Network synchronization measurement

For a collection of uncoupled neurons, bursting at different times may occur in a non-coherent way. However, when they are connected with synapses, they can have a coherent behavior. It is worth noting that the coherent behavior here refers to their bursting phase synchronization rather than synchronization on a spiking time scale. But this does not substantially affect the approximate periodicity of the mean field dynamics. In fact, in most cases, the spiking within the bursting is not completely synchronized. In order to characterize the synchronization degree of the bursting neurons, we can also use the mean field of the ensemble, which is defined as

$$X(t) = \frac{1}{N}\sum_{i=1}^{N} v_i(t), \tag{17}$$

where N is the number of coupled neurons, $v_i(t)$ represents the transmembrane voltage for the i-th neuron at the time t.

We fix rewiring probability $p = 0.1$, amplitude of electric field $A_{\rm e} = 0.4$, and frequency $f = 6.2$, $k_1 = 0.001$, and $k_2 = 0.001$. With the increase of coupling intensity η between the neurons, a transition to bursting phase synchronization is

observed. When the coupling intensity $\eta = 0$, the correlation of bursting behavior at different times in the small-world network is very weak, and the discharge rhythm of the network becomes very irregular (Fig. 2(c)). The mean field of excitatory neurons exhibits random fluctuation with a small amplitude (Fig. 2(b)). When the coupling intensity increases to $\eta = 5$, the discharge rhythm of the network becomes very regular (Fig. 2(f)). Both E-cells and I-cells show their bursting phase synchronization respectively. At this time, the mean field of excitatory neurons exhibits significant periodic oscillation (Fig. 2(e)). Here we can also observe that the cluster discharges of E-cells and I-cells present almost out-of-phase bursting synchronization. Therefore, it can be seen that the large periodic oscillation of the mean field characterizes the bursting phase synchronization, while random fluctuation with a small amplitude means that the bursting of coupled neurons is not synchronized. Because a state of synchronized bursting is characterized by a large-amplitude oscillation of mean field and random fluctuation with a small amplitude represents the absence of synchronization, we can use the variance of mean field oscillation $\mathrm{Var}(X)$ to measure the degree of synchronization of the network.

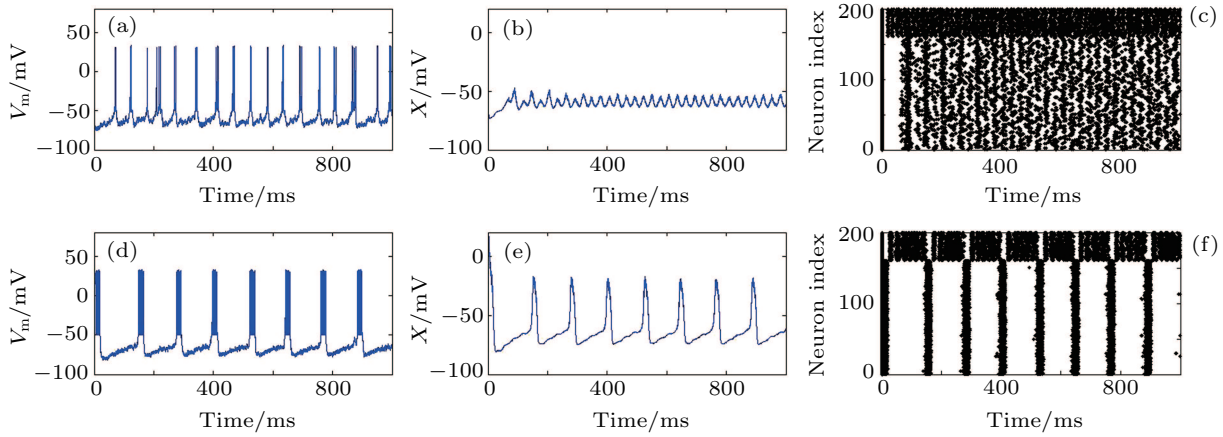


Fig. 2. (color online) ((a) and (d)) Time series for membrane potentials of a randomly selected E-cell in a small world network with $\eta = 0$ (a) and 5 (d); ((b) and (e)) mean fields of E-cell with $\eta = 0$ (b) and 5 (e); ((c) and (f)) spatiotemporal patterns of the network with $\eta = 0$ (c) and 5 (f).

2.5. Different types of neuron respond to localized signals

Previous studies have shown that the stochastic resonance phenomenon of the neural network induced by localized periodic signal stimulation is more remarkable than that of the periodic signal loading on all neurons. Here, we introduce a localized periodic signal stimulation in the form $I = A * \sin(\omega t)$, which is loaded additively into neurons in the network as a pacemaker. Here, parameter A represents the amplitude of the external forcing current, and ω is the corresponding frequency. Because the excitatory neuron population accounts for 80% of the total, we only consider the discharge characteristics of excitatory neurons population in the following discussion.

To quantitatively characterize the correlation between temporal output series of each excitatory neuron ${v_e}^i$ and the frequency of the pacemaker f, we calculate the Fourier coefficient Q^i according to Ref. [28], which is defined as

$$Q_{\sin}^{(i)} = \frac{1}{T}\sum_{t=1}^{T} 2{v_e}^i(t)\sin(\omega t), \tag{18}$$

$$Q_{\cos}^{(i)} = \frac{1}{T}\sum_{t=1}^{T} 2{v_e}^i(t)\cos(\omega t), \tag{19}$$

$$Q^{(i)} = \sqrt{{Q_{\sin}^{(i)}}^2 + {Q_{\cos}^{(i)}}^2}, \tag{20}$$

where T is the iteration step, and also the operation period of the pacemaker. We know that the Fourier coefficients are proportional to the square of the spectral power amplification, which is often used to measure stochastic resonance or the system output in a linear response to the input signal frequency ω. We use the average value of all $Q^{(i)}$ as a resonance factor, i.e., $Q = {N_e}^{-1}\sum_{i=1}^{N_e} Q^{(i)}$. In the following calculation, we take $T = 10^6$. To eliminate the influence of system random factors, the final result presented in the figures below is gained by averaging Q over 20 different realizations of each network.

Fixing parameter values $A = 0.1$, $\omega = 2\pi$, $\eta = 10$, $A_e = 0.1$, $f = 6.28$ and the other parameters remain unchanged, we randomly select the same number of E-cells and I-cells, and load this sinusoidal forcing current on these selected neurons, respectively. The collective behaviors of the systems for different types of neurons are depicted in Fig. 3(a). We can notice that when local signals are loaded into E-cells, the excitatory neurons show a synchronized bursting discharge activity. However, when the inhibitory neurons that are the same as the excitatory neurons in number receive the periodic signal, the population of excitatory neurons is in a subthreshold membrane potential oscillation state. Figure 5(a) also shows the dependence of Q on the number of neurons that receive the signal. This indicates that excitatory neurons in the network play an important role in receiving and detecting signals, and inhibitory neurons play a regulatory role in this process.

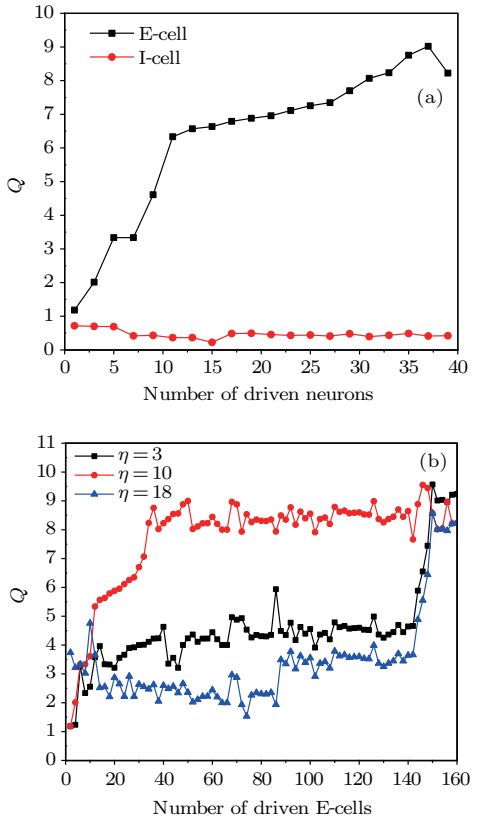


Fig. 3. (color online) (a) Resonance factor Q versus the number of driven neurons for different types of neurons and (b) the dependence of Q on the number of excitatory neurons that receive the local signal for different values of coupling strength η.

Figure 3(b) shows the dependence of Q on the number of excitatory neurons that receive the local signal for different values of coupling strength η. For coupling strength $\eta = 10$, it can be seen that the value of Q increases first, then stays the same with the increase of the number of excitatory neurons receiving signals. This result indicates that the collective dynamics of the system caused by a small number of neuron receptions is similar to that of a large number of neurons receiving signals, i.e, in the process of signal detection and information propagation, only a small number of neurons are required to receive signals to trigger an accurate response to input signals in the small world network. For too large values of coupling strength η, even local signal can activate the network synchronization activity, but the correlation between the temporal output series of each excitatory neuron and the frequency of the pacemaker ω is very poor. Moreover, a small coupling strength η may fail to evoke the discharge of other neurons in the network and the discharge synchronization activity of the whole network can be activated only when the coupling strength exceeds a certain threshold.

In fact, small values of coupling strength η make the interactions between neurons in the network weaker as if these neurons were a set of separate neurons. In this case, the neurons that do not receive signals in the network fail to produce action potential due to a lack of sufficient synaptic stimulation. That is to say, because of the small strength of the connection, these neurons cannot benefit from their neighbors, so localized rhythmic activity cannot effectively transmit across the network. On the other hand, a large coupling strength makes all neurons of the ensemble act as a single unit, so that the synchronous discharge of the network is due to the structure of the network itself, rather than the frequency of external stimulation. Both cases result in a poor correlation between temporal output series and the frequency. Therefore, the structure of the network has an important influence on the efficiency of the transmission of local signals. It seems that only the proper network parameters can balance the effectiveness and completeness of the signal transmission across all coupled units.

3. Results

3.1. Effect of induced electric field on synchronization

Since the network presents complex dynamical behaviors in electrical activities under different conditions, it is interesting to study the collective response of an E-I small world network exposed to an induced electric field generated by magnetic stimulation. Next, we will investigate the effect of an induced electric field on the bursting phase synchronization of the E-I small world network. We fix coupling intensity $\eta = 0.1$, amplitude of electric field $A_e = 2$, and the other parameters remain unchanged. Figure 4 shows the spatiotemporal patterns of this E-I small world network obtained for different values of frequency f. It can be seen that the frequency of the external field has an important influence on the transition of network bursting phase synchronization. When $f = 0.1$, the discharge rhythm of the network is very cluttered and the mean field of E-cells exhibits small-amplitude random fluctuation as shown in Fig. 4(a). Increasing the frequency to $f = 3.14$, the excitatory neurons in the network are in a bursting synchronization state, while the discharge rhythm of inhibitory neurons is not regular as shown in Fig. 4(b). Continue to increase the frequency $f = 6.28$, then all the neurons in the network will get bursting synchronization (Fig. 4(d)). As the frequency increases further, the synchronization state of the system disappears at $f = 8$ (Fig. 4(e)) and reappears at $f = 12.56$ (Fig. 4(f)). Figure 4(f) shows the evolution of $\mathrm{Var}(X)$ with f by different values of p. We can see that the greater the rewiring probability, the greater the maximum value of $\mathrm{Var}(X)$ is, that is to say, a larger p allows the system to achieve greater synchronization. The above results show that the frequency of the external field can promote or destroy the synchronous discharge behavior of the small world network with mixed synaptic connections, which can trigger a transition of the synchronization state. In addition, it can also be observed that with the increase of the frequency that is able to trigger the network synchronization, system synchronization gradually changes from merely excitatory neuron synchronization to a global network synchronization, and synchronous oscillation frequency becomes larger and larger.

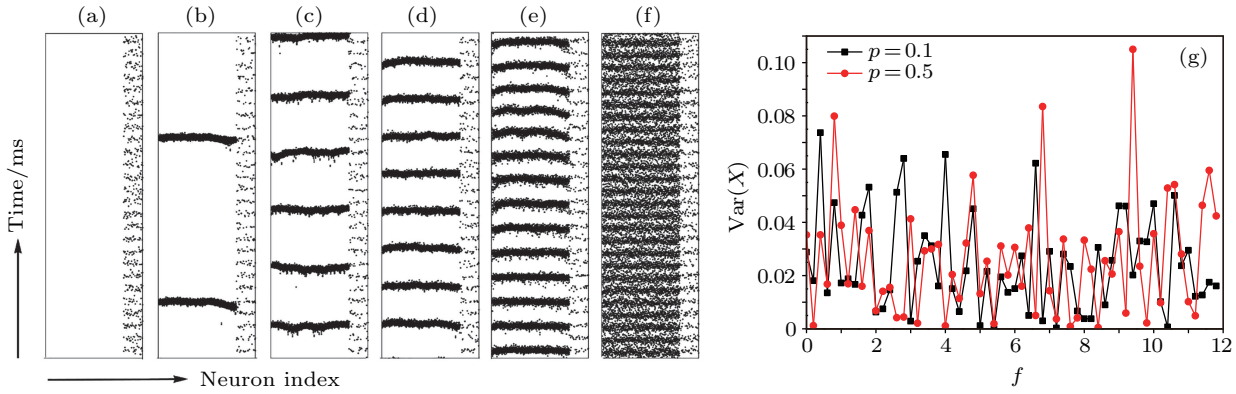


Fig. 4. (color online) (Left) Spatiotemporal patterns of the network obtained by different frequencies of AC electric field at $f = 0.1$ (a), 3.14 (b), 5 (c), 6.28 (d), 8 (e), and 12.8, (f). (Right) Variations of mean field Var(X) with electric field frequency f.

Figure 5 (left) shows the discharge rhythm of the E-I small world network with different electric field intensity at the time when the stimulus frequency $f = 6.28$. It is obvious that the intensity of the external field has an important influence on the bursting synchronization of the network. When $A_e = 0.1$, the collective electrical activity of the system is very messy (Fig. 5(a)). With the increase of the amplitude of the electric field, the collective electrical activity becomes more and more synchronized. Unlike the case of frequency change, the discharge rhythm of a neuron in the network is either in a disorganized state or in a bursting synchronization state, rather than only the excitatory neurons are in bursting synchronization. Next, we detect the effect of A_e on Var(X). Since rewiring probability p and external electric field frequency f may affect the dependence of the mean field variance on electric field strength, we depict the values of the variance of mean field Var(X) versus the electric field amplitude A_e for different values of p and f in Fig. 5(d). Fixing $f = 6.28$, we can observe that smaller A_e can cause network synchronization. At the beginning, as the amplitude of the electric field increases, the variance Var(X) increases rapidly and then slowly. For a smaller stimulus frequency $f = 3.14$, however, the smaller electric field amplitude A_e cannot cause network synchronization, only when the electric field intensity exceeds a certain threshold can the system produce the synchronous discharge activity, and then, with the increase of electric field intensity, the synchronicity of the network becomes stronger and stronger. In addition, too small frequency fails to evoke any synchronous discharge of the network, no matter how strong the electric field amplitude is. It is worth noting that the rewiring probability p does not affect the dependence of the mean field variance on electric field strength at a fixed external electric field frequency. These results show that the electric field can induce the transition of the network synchronization state, and when the intensity of the electric field is larger or the frequency takes some value, the neuron population shows abnormal synchronous discharge behavior. This may explain why electromagnetic radiation can cause some diseases.

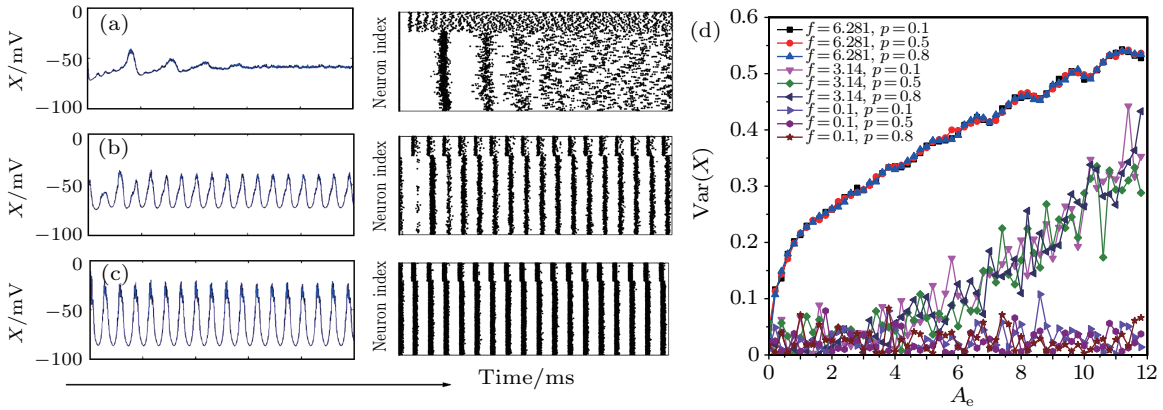


Fig. 5. (color online) (Left) Mean field $X(t)$ and spatiotemporal patterns of the network obtained by different amplitudes of AC electric field when $f = 6.28$, and $A_e = 0.01$ (a), 1 (b), and 4 (c). (Right) Variations of mean field Var(X) with electric field amplitude A_e for different values of rewiring probability p and frequency f.

3.2. Influence of magnetic flow on detection of weak signals

By remembering the magnetic flux across the membrane, memristor $\rho(\varphi)$ can be used to describe the memory effect, which is analogous to the autapse connection of the network. Moreover, the magnetic flux across the membrane on the neuronal system can change collective behaviors of neuronal networks and signal propagation. Now, we study the influence of

magnetic flux on the detection of weak signals in small world networks. According to the localized periodic signal described above, $I = A * \sin(\omega t)$, we introduce a localized weak periodic signal. We take $A = 0.001$, which can make sure that the pacemaker is subthreshold without other external stimuli. That means that it cannot lead to the neurons large-amplitude spikes by itself. We add this weak periodic signal to an excitatory neuron randomly selected, set the parameter values $\eta = 2$ and $p = 0.1$, and keep the other parameters unchanged. Since the effect of magnetic flow on membrane potential is described by imposing additive memristive current $(k_1\rho(\varphi)v)$ on the membrane variable, we take the intensity of interaction k_1 between membrane potential and magnetic flux as a control parameter to describe the effect of magnetic flow.

Figure 6 shows the spatiotemporal patterns and the mean fields of the E-cell ensemble of the network obtained for different intensities of interaction k_1. It can be seen that the no-flux boundary condition being used or a very small intensity of interaction $k_1 (< 0.0003)$ may fail to trigger any large-amplitude excitations (Fig. 6(a)), nor evoke only a few random ones and the distribution of the action potential is sparse (Figs. 6(b) and 6(c)). When the intensity of interaction is moderate, such as $k_1 = 0.0025$, temporal dynamics of each E-cell unit tends to be regularized and follows the rhythmic activity of this pacemaker (Fig. 6(d)). While a larger intensity of interaction k_1 can lead to spontaneous excitations, which are no longer consistent with the frequency of the pacemaker and the randomness is significantly enhanced (Fig. 6(f)). These phenomena show that the electric activity of a system triggered by a pacemaker appears to be rather irregular for large intensity of interaction k_1, and relatively regular electric activity appears when appropriate magnetic flux is applied to the membrane potential.

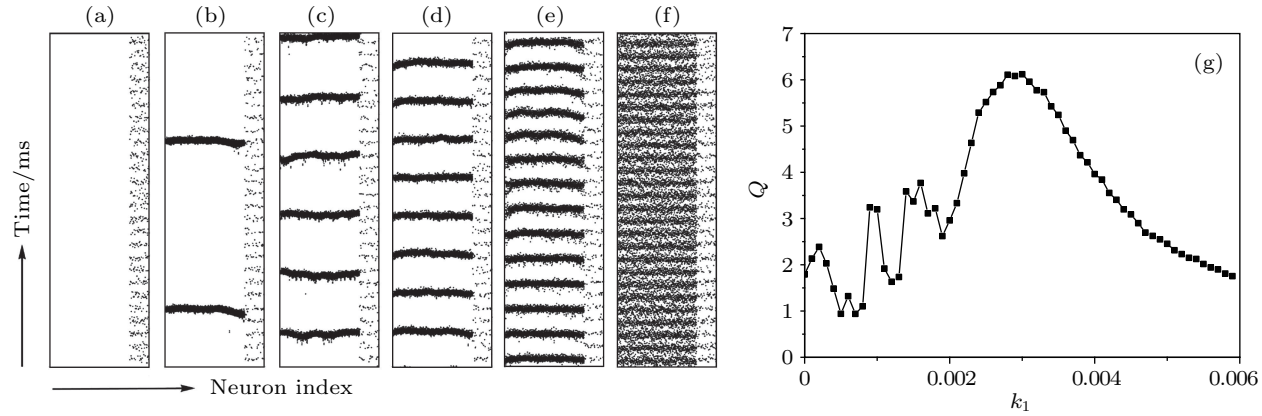


Fig. 6. (Left) Spatiotemporal patterns of the small-world network obtained by different electromagnetic induction intensities in the cases of (a) zeroed electromagnetic induction, $k_1 = 0.0001$ (b), 0.0005 (c), 0.001 (d), 0.0025 (e), and 0.004 (f). (g) Dependence of Q on interaction intensity k_1.

In order to gain more insights into the influences of electromagnetic induction on the weak periodic signal detection and information dissemination in neural systems, we calculate the dependence of Q on interaction intensity k_1 by using seven different values of coupling strength η, and keeping other parameters unchanged. The obtained results are shown in Fig. 7(a), when the coupling intensity is not very high (less than 2), there is an intermediate value of interaction strength k_1 at which Q is maximal for each particular coupling strength ω. Moreover, the maxima obtained in different cases are concentrated in the case where k_1 is between 0.002 and 0.003. It is worth noting that when the coupling intensity ω is too high (more than 10), the increase of electromagnetic induction intensity does not enhance the response of the system to weak periodic signal. These results indicate that neurons produce a discharge response to the weak periodic signal only when an appropriate magnetic flux is applied to the membrane potential, thus achieving accurate detection and transmission of weak periodic signals. A strong interaction k_1 can cause the regularity of the neuron action potential to be poor, so that the weak external periodic stimulus signal is blocked.

Since the frequency tuning is important in weak periodic signal detection and information transmission, we study the effects of different frequencies of weak stimulus signals on the global outreach of pacemakers. We calculate the dependence of Q on pacemaker frequency f by using three different values of electromagnetic induction intensity k_1. Results are presented in Fig. 7(b), from which it can be seen that the relationships between Q and pacemaker frequency ω are very different for different electromagnetic induction intensities, especially, the Q values in the three states have obvious boundaries. When the electromagnetic induction is less intense $(k_1 = 0.0001)$, Q exhibits random fluctuation with a large amplitude as the frequency increases, and the range of fluctuations is concentrated between 1 and 2.5. When the electromagnetic induction intensity is greater $(k_1 = 0.001)$, Q also shows the state of random fluctuation with the increase of pacemaker frequency. However, compared with the case of $k_1 = 0.0001$, its fluctuation range is small, but the total value of Q is large (between 3 and 4.5). When the electromagnetic induction intensity is too large $(k_1 = 0.004)$, Q also shows irregular oscillations of small amplitude, the amplitude is concentrated between 2.75 and 3,

which can be regarded as invariable. The electromagnetic radiation on the biological neuronal system has important influences on the detection of weak signals and information of the neuron system. It may determine the response degree of the biological system to the weak external signal.

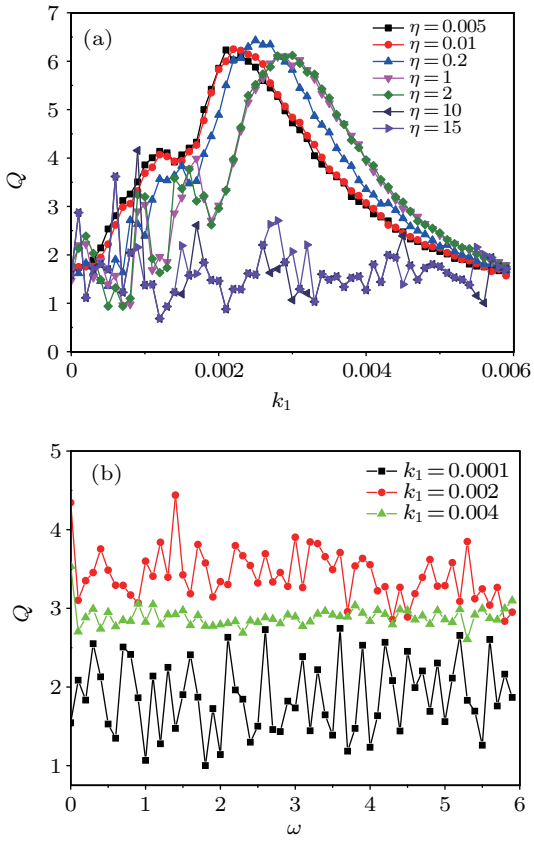


Fig. 7. (color online) (a) Variations of Q with electromagnetic induction intensity k_1 for different values of coupling strength η. (b) Variations of Q with frequency of weak stimulus signal for different values of electromagnetic induction intensity k_1 at $\eta = 0.02$.

3.3. Influence of electromagnetic induction on stochastic resonance

The phenomena of stochastic resonance on many neuronal networks, especially the excitatory systems, have been extensively studied recently.[41,42] It has been shown that the response of a nonlinear system to a weak signal exhibits a resonance dependence on the intensity of noise.[43] Wang *et al.* found that the effect of pacemaker-driven stochastic resonance depends extensively on network structure, such as rewiring probability, and coupling strengths.[30] Here, memristor $\rho(\varphi)$ can be used to describe the memory effect of the neuronal system, which has important influences on collective electrical activity and signal transmission; therefore, in what follows, we will examine the dependence of pacemaker-driven stochastic resonance of the network on the electromagnetic induction intensity on the neuronal system, which can be measured by the interaction between $\rho(\varphi)$ and membrane potential k_1. Figure 8(a) shows the dependence of Q on k_1 for a given noisy intensity $\sigma = 0.2$. We can see that as k_1 increases, Q first increases, then decreases. Moreover, there exists a pronounced maximum, which indicates the existence of an optimal electromagnetic induction intensity for the transmission of localized electrical activities.

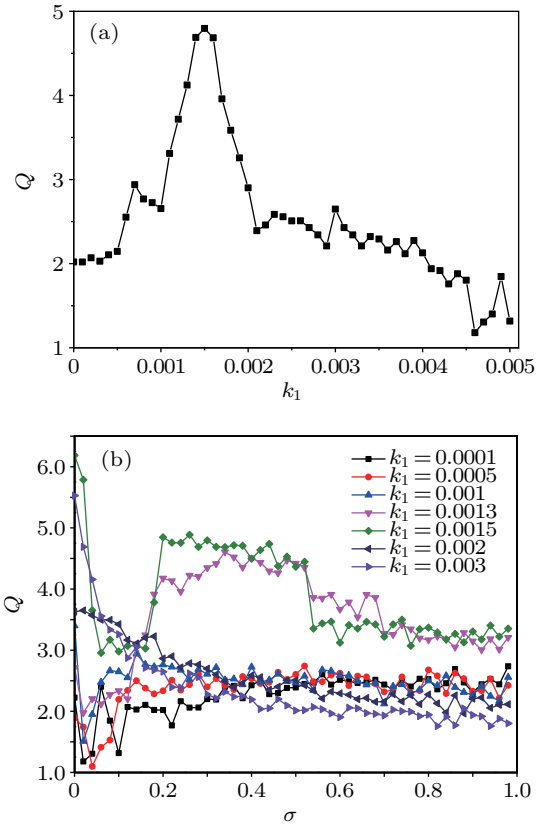


Fig. 8. (color online) (a) Dependence of Q on electromagnetic induction intensity k_1 for a given noisy intensity $\sigma = 0.2$. (b) Dependence of Q on noisy intensity σ for different values of electromagnetic induction intensity k_1.

In order to systematically analyze the effect of electromagnetic induction on the outreach of the subthreshold pacemaker, we calculate the temporal correlation between noisy intensity σ and system accurate response Q by using seven different values of k_1, and keep other parameters unchanged. As shown in Fig. 8(b), it can be seen that when the electromagnetic induction intensity is very small, no matter how the noise intensity changes, the stochastic resonance phenomenon of the nervous system cannot be induced. When the electromagnetic induction intensity is very large, a smaller noise intensity can trigger stochastic resonance. However, as the noise intensity increases, the value of Q decreases rapidly, and it fails to evoke the system response. Therefore, only in the case of moderate electromagnetic induction (k_1 is 0.0013 or 0.0015) does there exist some suitable noise intensity, which makes the stochastic resonance appear.

At the same time, we can also observe that the Q decreases with the increase of the noise intensity, then study the maximum steady-state value, which oscillates at the steady-state value and then oscillates with decay, and finally stabilizes at a certain value. Wang *et al.* found that there exists an

intermediate value of noisy intensity σ at which Q is a peak value for each particular coupling strength or rewiring probability. However, unlike their conclusions, our results show that there is a certain range of noise intensity rather than a single intermediate value, which makes Q a larger value in this range. This result indicates that under the influence of electromagnetic induction, there is a large range of noise intensity to make the system generate random resonance phenomenon. Therefore, we can conclude that the subthreshold pacemaker is easier to extend in the network and the system is easier to detect external weak signals in the appropriate electromagnetic induction.

4. Conclusions

In this paper, using the E-I small world network we built, we first investigate the influence induced electric field on the bursting phase synchronization of the E-I small world network. We find that the external field has an important influence on the transition of network bursting phase synchronization. When the intensity of the electric field is large enough or the frequency is taken to be some value, the neuron population shows abnormal synchronous discharge behavior. We then explore the responses of different types of neurons to periodic signals in the network, and find that excitatory neurons in the network play an important role in recepting and detecting signals. Moreover, the effects of the number of excitatory neurons that receive the local signal on resonance factor Q under different coupling intensities are detected. It is shown that only a small number of neurons in the small world network are required to receive signals that can trigger an accurate response to the input signal, and the structure of the network has an important influence on the efficiency of the transmission of local signals. On the other hand, we analyze the effect of magnetic flow on the localized weak periodic signal detection and information dissemination in neural systems. We show that neurons produce a discharge response to the weak periodic signal only when an appropriate magnetic flux is applied to the membrane potential. Finally, we demonstrate the influence of magnetic flux on stochastic resonance, and find the existence of an optimal intensity of interaction (k_1) for the transmission of localized electrical activities, that is to say, a subthreshold pacemaker is easier to extend in the network and the system is more likely to detect external weak signals under the appropriate magnetic flux. For now, the effects of induced electric field generated by magnetic stimulation and magnetic flux across the membrane on collective electrical activities and signals propagation have been investigated. We hope that our findings will help promote further development of transcranial magnetic stimulation (TMS), which is a noninvasive procedure for treating certain neurological diseases.

References

[1] Hodgkin A L and Huxley A F 1990 *Bull. Math. Biol.* **52** 25
[2] Morris and Lecar 1981 *Biophys. J.* **35** 193
[3] Zhang J, Huang S, Pang S, Wang M and Gao S 2015 *Chin. Phys. Lett.* **32** 120502
[4] Rulkov N F, Timofeev I and Bazhenov M 2004 *J. Comput. Neurosci.* **17** 203
[5] Shi X and Lu Q 2005 *Chin. Phys. B* **14** 77
[6] Gu H, Pan B, Chen G and Duan L 2014 *Nonlinear Dyn.* **78** 391
[7] Izhikevich, E M 2004 *IEEE Trans. Neural Networks* **15** 1063
[8] Lv M, Wang C, Ren G, Ma J and Song X 2016 *Nonlinear Dyn.* **85** 1479
[9] Lv M and Ma J 1981 *Biophys. J.* **205** 375
[10] Han F, Wang Z, Fan H and Gong T 2015 *Chin. Phys. Lett.* **32** 040502
[11] Gu H, Pan B and Li Y 2015 *Nonlinear Dyn.* **82** 1191
[12] Gu H, Chen S G, Curtu R and Li Y2015 *Chin. Phys. B* **24** 050505
[13] Ventriglia F 2008 *Cognitive Neurodynamics* **2** 335
[14] Cheyne D, Bells S, Ferrari P, Gaetz W and Bostan A C 2008 *Neuroimage* **42** 332
[15] Koenig T, Prichep L, Dierks T, Hubl D, Wahlund L O, John E R and Jelic V 2005 *Neurobiology of Aging* **26** 165
[16] Gorsev G, Y and Erol B 2010 *Cognitive Neurodynamics* **4** 263
[17] Wilson T W, Rojas D C, Reite M L, Teale P D and Rogers S J 2007 *Biological Psychiatry* **62** 192
[18] Wang R, Zhang Z, Qu J and Cao J 2011 *IEEE Trans. Neural Networks* **22** 1097
[19] Jiao X and Wang R 2010 *Int. J. Nonlinear Mech.* **45** 647
[20] Yuan L, Liu Z, Zhang H, Ding X, Yang M, Gu H and Ren W 2011 *Chin. Phys. B* **20** 020508
[21] Li H and Wang Y 2014 *Acta Phys. Sin.* **63** 120506 (in Chinese)
[22] Yu H, Wang J, Liu C, Che Y, Deng B and Wei X 2012 *Acta Phys. Sin.* **61** 068702 (in Chinese)
[23] Gong Y, Wang M, Hou Z and Xin H 2005 *Chemphyschem* **6** 1042
[24] Gao Z, Hu B and Hu G 2002 *Phys. Rev. E* **65** 016209
[25] Ozer M, Perc M, Uzuntarla M and Koklukaya E 2010 *Neuroreport* **21** 338
[26] Bezrukov S M and Vodyanoy I 1995 *Nature* **378** 362
[27] Levin Amp J E and Miller J P 1996 *Nature* **380** 165
[28] Perc M 2007 *Phys. Rev. E* **76** 066203
[29] Ozer M, Perc M and Uzuntarla M 2009 *Phys. Lett. A* **373** 964
[30] Yu H, Wang J, Liu C, Deng B and Wei X 2011 *Chaos* **21** 047502
[31] Pashut T, Wolfus S, Friedman A, Lavidor M, Bargad I, Yeshurun Y and Korngreen A 2011 *Plos Comput. Biology* **7** e1002022
[32] Devos D and Defebvre L 2006 *Prog. Brain Res.* **159** 331
[33] Ma J, Wu F and Wang C 2017 *Int. J. Mod. Phys. B* **31** 391
[34] Watts D J and Strogatz S H 1998 *Nature* **393** 6684
[35] Izhikevich E M 2003 *IEEE Trans. Neural Networks* **14** 1569
[36] Bedard C, KroGer H and Destexhe A 2006 *Phys. Rev. E* **73** 051911
[37] Gianni M, Liberti M, Apollonio F and Inzeo G 2006 *Biological Cybernetics* **94** 118
[38] Bao B C, Liu Z and Xu J P 2010 *Electron. Lett.* **46** 237
[39] Li Q, Zeng H and Li J 2015 *Nonlinear Dyn.* **79** 2295
[40] Golomb D, Shedmi A, Curtu R and Ermentrout G B 2006 *J. Neurophysiology* **95** 1049
[41] Jung P, Behn U, Pantazelou E and Moss F 1992 *Phys. Rev. A* **46** R1709
[42] Jung P and Mayer-Kress G 1995 Phys. Rev. Lett. **74** 2130
[43] Mato G 1998 *Phys. Rev. E* **58** 876